H₃PO₃ electrochemical behaviour on a bulk Pt electrode: adsorption and oxidation kinetics

M. Prokop, T. Bystron*, M. Paidar, K. Bouzek

Department of Inorganic Technology, University of Chemistry and Technology Prague, Technicka 5, Prague 6, 166 28, Czech Republic

ABSTRACT

Polybenzimidazole-type polymer doped with H_3PO_4 is commonly used as the proton-conductive phase in high-temperature proton-exchange membrane fuel cells. However, H_3PO_4 is not stable during fuel cell operation and undergoes reduction by hydrogen on a Pt surface to phosphorus compounds in a lower oxidation state, such as H_3PO_3. In this work the kinetics of H_3PO_3 oxidation on Pt electrode was studied, including an investigation of $H_4P_2O_6$ as a possible oxidation intermediate. H_3PO_3 adsorption in hydrogen underpotential deposition region was described by a triple Langmuir isotherm corresponding to adsorption on specific Pt crystalline planes. Co-adsorption of hydrogen as well as SO_4^{2-}, HSO_4^- ions decreased the total amount of adsorbed H_3PO_3. The determined apparent charge transfer coefficients of H_3PO_3 anodic oxidation on a metallic Pt surface were found to be concentration and temperature-dependent, indicating that the nature of the anodic process is complex. From chronopotentiometric measurements of H_3PO_3 and $H_4P_2O_6$ oxidation on a preoxidised Pt surface it was concluded that, while H_3PO_3 is oxidised by means of a chemical reaction with PtO_x, $H_4P_2O_6$ undegoes anodic oxidation on the PtO_x surface. According to voltammetry and bulk electrolysis experiments $H_4P_2O_6$ is not formed as an intermediate product during electrochemical oxidation of H_3PO_3 on a metallic Pt surface.

© 2016 Elsevier Ltd. All rights reserved.

1. Introduction

Fuel cells represent one of the vital devices for energy conversion in the hydrogen economy scheme [1]. Of all the various types, high temperature fuel cells with a proton-exchange membrane (HT PEM FC) are one of the most promising options due to their operating temperature of 120–200 °C and consequently relatively high resistance to CO poisoning along with reasonable material demands. On the other hand, such an operating temperature requires the use of membranes based on a polybenzimidazole-type polymer doped with H_3PO_4 [2]. The negative effects of H_3PO_4, including adsorption on Pt nanoparticles and the impact on O_2 reduction reaction kinetics, have already been described in numerous studies [3–6]. Although not frequently mentioned, the stability of H_3PO_4 under conditions corresponding to HT PEM FC operation is also an issue [7,8]. Information on the reduction of H_3PO_4 to phosphorus compounds in a lower oxidation state and their impact on the Pt catalyst is, however, still not consistent.
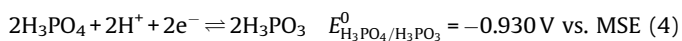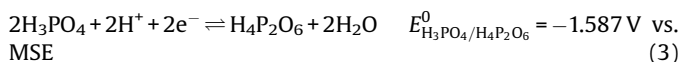
The oxidation of phosphorus impurities, present at elevated temperatures in concentrated H_3PO_4, on Pt electrode has been reported by several authors [7,9–11]. These impurities strongly adsorb on a Pt surface. Their formation takes place at potentials corresponding to hydrogen adsorption, evolution and their anodic oxidation proceeds at potentials in the double layer region. The exact nature of these impurities has been a matter of discussion for a long time. In the work of Vogel and Baris these compounds were assumed to be H_3PO_4 reduction products, namely Pt-P [7]. Sugishima et al. extended the state of knowledge by suggesting that H_3PO_3 was one of the impurities [10]. In their following work the negative influence of H_3PO_3 on a Pt electroactive surface was described as well as the fact that H_3PO_3 oxidation is a competitive reaction to O_2 reduction [12]. The presence of Pt-P and H_3PO_3 impurities on a Pt surface during polarization of a H_3PO_4-doped membrane at a temperature of 125 °C was confirmed by Doh et al. using scanning photoelectron microscopy [13]. The formation of impurities was ascribed to the electrochemical reduction of H_3PO_4 as well as to its chemical reduction by H_2, with Pt acting as the catalyst of these processes. A brief study of the electrochemical behaviour of H_3PO_3 on Pt was published by Bravacos et al. and Trasatti et al. [14,15]. In the work of Prokop et al. both the electrochemical behaviour of H_3PO_2 and H_3PO_3 and the surface

---

* Corresponding author. Tel.: +420 220 444 272.
E-mail addresses: prokopm@vscht.cz (M. Prokop), bystront@vscht.cz
(T. Bystron), paidarm@vscht.cz (M. Paidar), bouzekk@vscht.cz (K. Bouzek).

coverage of Pt by these phosphorus oxoacids were examined. According to this work, H_3PO_3 surface coverage of Pt increases with rising temperature [11]. This unusual phenomenon was explained by the tautomeric equilibria between a thermodynamically more stable "inactive" tetrahedral and a strongly adsorbing "active" pyramidal form of the acid [16–18].

Baudler and Schellenberg studied the electrochemical oxidation of various phosphorus oxoacids as well as the H_3PO_4 reduction mechanism on Pt and other metal electrodes. According to their findings the oxidation of H_3PO_3 could proceed with a P(IV) compound as an intermediate [19]. $H_4P_2O_6$ is a white crystalline compound that is stable at ambient temperature in the form of $H_4P_2O_6 \cdot 2H_2O$. Hydrated hypophosphates, e.g. $Na_2H_2P_2O_6 \cdot xH_2O$ (x = 6, 10), are also known. In aqueous solutions $H_4P_2O_6$ behaves as a weak tetrabasic acid (pKa$_1$ = 2.2, pKa$_2$ = 2.8, pKa$_3$ = 7.3, pKa$_4$ = 10.0) [20]. Therefore, hypophosphates undergo protonation to $H_4P_2O_6$ in strongly acidic aqueous solutions. The prolonged presence of $H_4P_2O_6$ in a strongly acidic environment and at elevated temperatures leads to its disproportionation to H_3PO_3 and H_3PO_4 according to Eq. (1). The standard redox potentials of $H_4P_2O_6/H_3PO_3$ and $H_3PO_4/H_4P_2O_6$ couples are indicated in Eqs. (2) and (3). The standard redox potential of H_3PO_4/H_3PO_3 is included in Eq. (4) for comparison. Even at ambient temperature and when anhydrous, $H_4P_2O_6$ with a P(IV)-P(IV) bond undergoes a slow rearrangement to form isohypophosphoric acid, containing P(III)-O-P(V) bond, i.e. the two phosphorus atoms in different oxidation states are connected via an oxygen atom [20]. Isohypophosphoric acid is not stable and disproportionates to $H_4P_2O_7$ and $H_4P_2O_5$.

$$H_4P_2O_6 + H_2O \rightarrow H_3PO_3 + H_3PO_4 \qquad (1)$$

$$H_4P_2O_6 + 2H^+ + 2e^- \rightleftharpoons 2H_3PO_3 \quad E^0_{H_4P_2O_6/H_3PO_3} = -0.274 \text{ V vs. MSE} \quad (2)$$

$$2H_3PO_4 + 2H^+ + 2e^- \rightleftharpoons H_4P_2O_6 + 2H_2O \quad E^0_{H_3PO_4/H_4P_2O_6} = -1.587 \text{ V vs. MSE} \quad (3)$$

$$2H_3PO_4 + 2H^+ + 2e^- \rightleftharpoons 2H_3PO_3 \quad E^0_{H_3PO_4/H_3PO_3} = -0.930 \text{ V vs. MSE} \quad (4)$$

So far almost no information is available on H_3PO_3 oxidation kinetics, except for the work of Trasatti and Alberti who studied the kinetics of H_3PO_3 oxidation in 0.5 mol L^{-1} H_2SO_4 aqueous solution at 25 °C mainly on a bulk Pd electrode [21]. They proposed H_3PO_3 oxidation to a P(IV) product via catalytic dehydrogenation of H_3PO_3 on a Pd surface, followed by electrochemical oxidation of the adsorbed hydrogen. The catalytic dehydrogenation to the P(IV) compound was suggested as the rate-determining step. The P(IV) product subsequently disproportionates to H_3PO_3 and H_3PO_4 [21]. Trassati and Alberti also briefly studied H_3PO_3 oxidation on a Pt electrode, however no kinetic information was provided in their publication [15]. They suggested that H_3PO_3 oxidation on a Pt electrode proceeds by the same mechanism as on a Pd electrode. However, this conclusion was not supported by sufficient experimental data, and when large differences in hydrogen adsorption energies on Pt and Pd are taken into account (approximately −45 and −36 kJ mol^{-1} for Pd-H and Pt-H bond respectively) their theory still remains open [22,23].

The main goal of the present study is to extend the findings presented in our previous work [11], to include information on H_3PO_3 adsorption in the presence of SO_4^{2-}, HSO_4^- and ClO_4^- in the electrolyte solution. The kinetics of H_3PO_3 electrochemical oxidation will be determined for a polycrystalline Pt electrode and for 0.5 mol L^{-1} H_2SO_4 aqueous solution at various temperatures. Furthermore, the electrochemical behaviour of

hypophosphoric acid ($H_4P_2O_6$) as a possible H_3PO_3 oxidation reaction intermediate will be investigated.

2. Experimental

Extra pure chemicals, i.e. 98% phosphorous acid (Acros Organics, extra pure), 96% sulphuric acid (Fluka, for trace analysis), 85% phosphoric acid (Acros Organics, extra pure, SLR) and 70% perchloric acid (Acros Organics, for analysis) were used in the experiments. Crystalline $Na_2H_2P_2O_6 \cdot 10H_2O$ was synthesised using a method previously described by Remy and Falius [24]. The presence of crystalline $Na_2H_2P_2O_6 \cdot 10H_2O$ phase in the prepared sample was confirmed by means of X-ray diffraction using an X'pert PRO (PANanalytical, Netherlands) diffractometer. The purity of $Na_2H_2P_2O_6 \cdot 10H_2O$ was higher than 94% according to analyses performed by means of thermogravimetry on STA PT 700 LT (Linseis, Germany) with temperature scan rate of 10 °C min^{-1} from room temperature up to 170 °C, X-ray diffraction on X'pert PRO (PANanalytical, Netherlands) and ICP-OES on Optima8000 (Perki-nElmer, USA), while the remaining 6% probably correspond to excess water in the salt. Before the experiment the appropriate amount of $Na_2H_2P_2O_6 \cdot 10H_2O$ was dissolved in 0.5 mol L^{-1} H_2SO_4 or H_3PO_4 solution where $Na_2H_2P_2O_6$ undergoes protonation to $H_4P_2O_6$. All solutions were prepared from fresh deionised water (conductivity 0.2 μS cm^{-1}) made by the DIWA deionisation system (WATEK, Czech Republic). Before each measurement the equipment that would be in contact with the electrolyte and electrodes was rinsed with distilled water and then treated with 96% H_2SO_4: 30% H_2O_2 (1:3) "piranha" solution for at least 15 hours. After purification by "piranha" solution the equipment was thoroughly rinsed with deionised water.

A pyrex glass electrochemical cell (50 cm^3) tempered by a F12 cryostat (Julabo, Germany) was used for the experiments. The measurements were performed in a three-electrode arrangement. Pt foil (7 cm^2) and Hg/Hg$_2$SO$_4$ in K$_2$SO$_4$(sat.) solution (MSE) were used as the counter-electrode and reference electrode, respectively. All potentials in this paper refer to this reference electrode. The reference electrode was separated from the electrolyte by a double liquid junction, the first was filled with supporting electrolyte used in the electrochemical cell, the second with a saturated K$_2$SO$_4$ solution. The working electrode was planar Pt foil with a geometric area of 1.11 cm^2 and a roughness factor of about 1.25. Potentiostatic batch electrolysis was carried out in a three-electrode arrangement in a glass electrolytic cell with a Pt mesh (approx. 50 cm^2) working electrode and Pt wire counter-electrode separated from the electrolyte by a ceramic frit. The same reference electrode was used as in the voltammetry experiments. The electrolyte solution was agitated by a PTFE stirrer (cross-like shape, 2 cm wide, rotation speed 500 RPM). The applied potential was 0.1 V vs. MSE. Prior to each experiment the working electrode was rinsed thoroughly with deionised water and cycled for at least one hour between −0.7 and 0.9 V in corresponding electrolyte at a potential scan rate of 100 mV s^{-1} After cycling, the used electrolyte was replaced by a fresh one. All voltammetry measurements were performed with a HEKA PG310 potentiostat. All experimental voltammograms presented were corrected for the presence of background currents and iR drop in the electrolyte. The electrolyte pH was measured by an Easy Pro automatic titrator (Mettler Toledo, Switzerland) with an EM45-BNC sensor. The concentration of H_3PO_3 and H_3PO_4 in the electrolyte was analysed by a DIONEX ICS 1000 ion-exchange liquid chromatograph (Thermo Scientific, USA). An IonPac AS4A-SC 4 mm analytical column with an IonPac AG4A-SC 4 mm guard column and ASRS-ULTRA II (4 mm) anion self-regenerating supressor were used. The mobile phase was 1.8 mmol L^{-1} Na_2CO_3 + 1.7 mmol L^{-1} $NaHCO_3$ aqueous solution.

3. Results and discussion

3.1. Adsorption of H_3PO_3 on a Pt surface

Adsorption isotherms of H_3PO_3 determined in $0.5\,mol\,L^{-1}$ H_2SO_4 aqueous solution in the electrode potential range of hydrogen underpotential deposition on a polycrystalline Pt electrode presented previously in [11] were fitted using Athena Visual Studio with a Langmuir triple-adsorption model according to Eq. (5). The following assumptions were made: three independent types of adsorption sites are present on the electrode surface; H_3PO_3 adsorption on each type of adsorption site at constant electrode potential follows the Langmuir isotherm. The fitted values of equilibrium adsorption constants and maximum coverages are included in Table 1. Triple adsorption can be interpreted as independent adsorption of H_3PO_3 on three different low-index crystalline planes present on a bulk polycrystalline Pt electrode. The fitted isotherms, showing a good agreement with the experimental data, are presented in Fig. 1.

$$\theta = \frac{K_{ads,1}c}{K_{ads,1}c+1}\theta_{max,1} + \frac{K_{ads,2}c}{K_{ads,2}c+1}\theta_{max,2} + \frac{K_{ads,3}c}{K_{ads,3}c+1}\theta_{max,3} \qquad (5)$$

θ—partial surface occupation by H_3PO_3, c—H_3PO_3 concentration in $mol\,m^{-3}$, $K_{ads,x}$—equilibrium adsorption constant on a crystalline plane numbered x, $\theta_{max,x}$—maximum partial surface occupation on crystalline plane x. It is assumed that $\theta_{max,1} + \theta_{max,2} + \theta_{max,3} = 1$. Here, the partial surface occupation θ is defined as a fraction of the Pt electrode surface covered by the studied adsorbent (the remaining part of the surface, $1 - \theta$, is not covered by the studied adsorbent). Such a quantity does not allow one to distinguish between mono- and multilayer adsorption. It is thus not to be confused with surface coverage.

The effect of co-adsorbing H, SO_4^{2-}, HSO_4^- and ClO_4^- on H_3PO_3 adsorption on a Pt surface was examined by cyclic voltammetry using varying lower reversal potential in $0.5\,mol\,L^{-1}$ H_2SO_4 and $HClO_4$ aqueous solutions with an addition of H_3PO_3. Aqueous H_2SO_4 solution was chosen as a supporting electrolyte for continuity with previous experiments, while $HClO_4$ represents a non-adsorbing electrolyte for comparison purposes. During the experiment, an electrode potential was scanned from a fixed starting potential ($-0.25\,V$) to a more negative lower-reversal potential where H_3PO_3 adsorbs and then a potential was scanned to positive electrode potentials in order to oxidise H_3PO_3 present in the vicinity of the electrode. This oxidation process is on the voltammograms visible as the peak pα [11], see Fig. 2. Peak pα' resulting from H_3PO_3 oxidation on Pt surface freed from oxides during negative going potential scan was not used for study due to non-defined conditions of H_3PO_3 adsorption. The objective of these experiments was to examine the influence of potential on the amount of adsorbed H_3PO_3. The evaluation was performed using the following treatment. First, the anodic charge $Q_{Ox,i}$ in C was obtained by the current (measured during the positive going sweep) integration in the potential region between -0.2 and $0.8\,V$ for each voltammogram. As one can see from the voltammograms presented in Fig. 2, the only differences in these parts of voltammetry curves are due to variation of oxidation peaks pα. Subsequently, the maximum charge $Q_{Ox,max}$ obtained within the
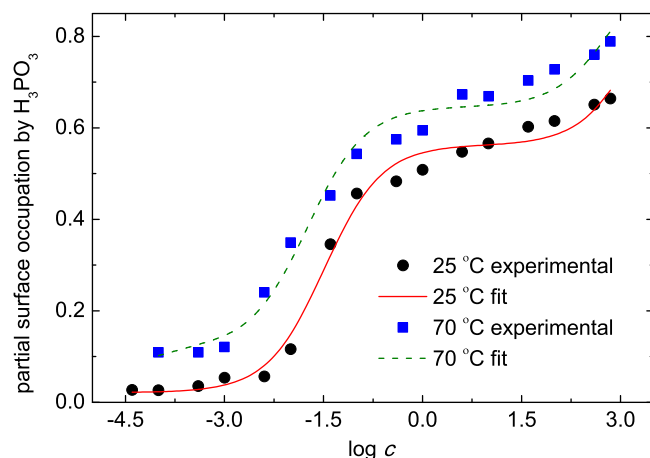

Fig. 1. H_3PO_3 adsorption isotherms on a polycrystalline Pt electrode in $0.5\,mol\,L^{-1}$ H_2SO_4 aqueous solution. The logarithm was calculated using concentrations in $mol\,m^{-3}$. Temperatures are included in plot inset.
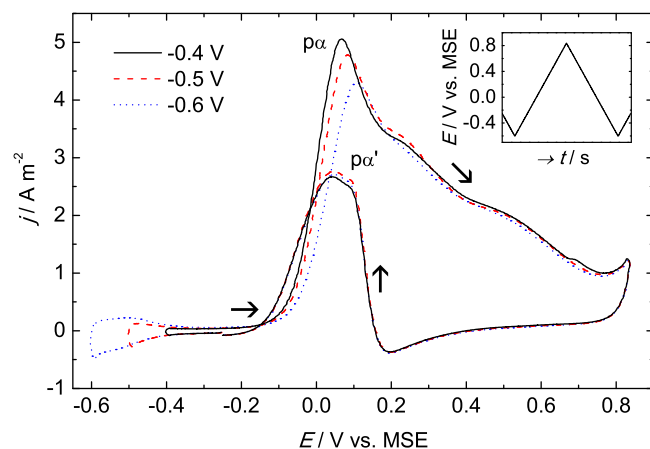

Fig. 2. Cyclic voltammetry of a polycrystalline Pt electrode in $0.5\,mol\,L^{-1}$ $H_2SO_4 + 1\,mmol\,L^{-1}$ H_3PO_3 at $70\,°C$. Electrolyte saturated with N_2. Scan description: $-0.25\,V \to$ lower reversal potential $\to 0.84\,V \to -0.25\,V$, potential sweep rate $50\,mV\,s^{-1}$. The value of the lower reversal potential is stated in the plot inset. Inserted plot shows evolution of electrode potential in time.

experimental series was selected from $Q_{Ox,i}$ values. The change in H_3PO_3 adsorbed amount expressed as number of monolayers desorbed $\Delta\theta_M$ (dimensionless) was determined using Eq. (6), z (= 2) is number of electrons removed per molecule of H_3PO_3, F (= $96\,485\,C\,mol^{-1}$) is Faraday constant, Γ_{Pt} (= $2.2 \cdot 10^{-5}\,mol\,m^{-2}$) is surface concentration of Pt atoms and $EASA$ in m^2 is electrochemically active surface area of the electrode determined by means of hydrogen underpotential deposition. The calculation of $\Delta\theta_M$ is based on Faraday law and, in principle, only allows one to evaluate changes in the extent of H_3PO_3 adsorption and not the total amount of H_3PO_3 adsorbed on the electrode surface.

$$\Delta\theta_M = \frac{Q_{Ox,i} - Q_{Ox,max}}{z \cdot F \cdot \Gamma_{Pt} \cdot EASA} \qquad (6)$$

In $0.5\,mol\,L^{-1}$ H_2SO_4 solution at $25\,°C$ the H_3PO_3 oxidation peak (and the amount of originally adsorbed H_3PO_3) was largest when the lower reversal potential had a value of approximately $-0.40\,V$ and it decreased when this potential was either more positive or negative, see Fig. 3. H_3PO_3 desorption was most pronounced in the potential region of hydrogen adsorption/evolution, resulting in a lower charge of the H_3PO_3 oxidation peak in the following positive-

Table 1
Equilibrium adsorption constants and maximal partial surface occupation by H_3PO_3 of polycrystalline Pt electrode in $0.5\,mol\,L^{-1}$ H_2SO_4 aqueous solutions saturated with N_2.

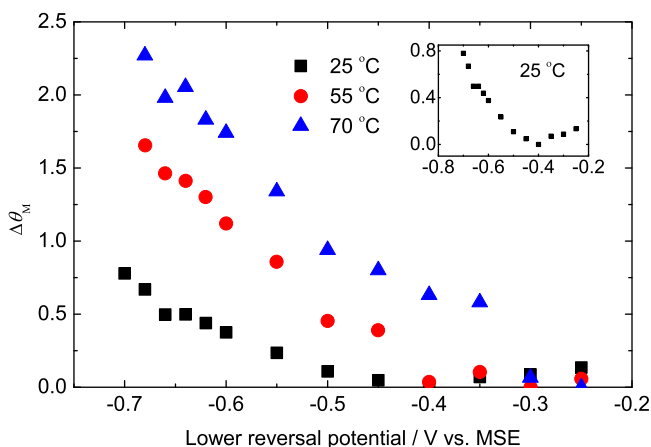| T / °C	$K_{ads,1}$	$\theta_{max,1}$	$K_{ads,2}$	$\theta_{max,2}$	$K_{ads,3}$
25	$3.5 \cdot 10^7$	0.022	$3.07 \cdot 10^1$	0.541	$5.39 \cdot 10^{-4}$
70	$4.5 \cdot 10^4$	0.121	$5.51 \cdot 10^1$	0.525	$1.25 \cdot 10^{-3}$

Fig. 3. Dependence of desorbed H_3PO_3 monolayers on lower reversal potential during cyclic voltammetry measurements in $0.5 \, mol \, L^{-1}$ H_2SO_4 aqueous solution with an addition of $1 \, mmol \, L^{-1}$ H_3PO_3 ($-0.25 \, V \rightarrow$ lower reversal potential $\rightarrow 0.84$ $V \rightarrow -0.25 \, V$), potential sweep rate $50 \, mV \, s^{-1}$. Electrolyte saturated with N_2. Electrolyte temperature is stated in the figure inset. Inserted plot shows detail of data recorded at temperature of $25 \, ^{\circ}C$.

going potential scan. The value of $-0.40 \, V$ coincides with the reported potential of zero charge ($-0.384 \, V$) of a Pt electrode in $0.5 \, mol \, L^{-1}$ H_2SO_4 at $25 \, ^{\circ}C$ [25]. The adsorption of H_3PO_3 in the form of an anion would lead to dramatic changes in the potential of zero charge value. It can thus be assumed that, in the system studied, H_3PO_3 was adsorbed on the Pt surface in the protonated form. This is also in agreement with our previous conclusions that it is the "active" $P(OH)_3$ form of H_3PO_3 that adsorbs on the Pt surface. Finally, it agrees with $P(OH)_3$ reported acido-basic properties ($pKa_1 = 7.4$). As the pH value of the studied solution was about 0.35, practically all $P(OH)_3$ molecules in the electrolyte were protonated [17].

At $25 \, ^{\circ}C$ the maximum desorption of 0.78 of a H_3PO_3 monolayer was observed when the lower reversal potential was shifted from -0.4 to $-0.7 \, V$. From the adsorption isotherm for $25 \, ^{\circ}C$, presented in Fig. 1 (determined from cyclic voltammograms with a lower reversal potential of $-0.65 \, V$, H_3PO_3 concentration of $1 \, mmol \, L^{-1}$) it is clear that, at a potential of $-0.65 \, V$, approximately 50% of the electrode surface is still covered by H_3PO_3. At the same time, desorption of about 0.5 monolayer at this potential, compared to $-0.4 \, V$, is visible in Fig. 3. Thus, the maximum amount of adsorbed H_3PO_3 observed at potentials around $-0.4 \, V$ attains at least 1 monolayer. According to the voltammograms similar to these presented in Fig. 2, the co-adsorption of H on the Pt surface at temperatures of 55 and $70 \, ^{\circ}C$ has a pronouncedly negative effect on the amount of H_3PO_3 adsorbed. At these temperatures the maximum amount of desorbed H_3PO_3 is equivalent to at least 1.7 and 2.3 monolayers, respectively. This corresponds to the situation when the lower reversal potential is lowered from about -0.25 to $-0.68 \, V$ (Fig. 3). If the information about the adsorption from Fig. 1 (isotherm at $70 \, ^{\circ}C$ determined from cyclic voltammograms with lower reversal potential of $-0.62 \, V$, H_3PO_3 concentration of $1 \, mmol \, L^{-1}$) and Fig. 3 (for $-0.62 \, V$) at a temperature of 70 $^{\circ}C$ is combined, it yields a value of about 2.3 monolayers. This is in agreement with the maximum amount of desorbed H_3PO_3 observed at $-0.68 \, V$ in Fig. 3 and it documents the agreement between the previous and the new published data. Surprisingly, the maximum amount of adsorbed H_3PO_3 largely exceeds the amount corresponding to the monolayer coverage. This is interesting because direct contact between the Pt surface and the "second" and "third" H_3PO_3 layers, required for chemisorption, is not possible. Therefore, it seems that at least part of the H_3PO_3 molecules is present on the Pt surface in the form of a polyacid

(mainly as $H_4P_2O_5$ and $H_5P_3O_7$ produced by condensation of "active" $P(OH)_3$ molecules). Their concentration in the electrolyte solution at a higher temperature increases, as already discussed in our previous work [11]. The presence of adsorbed polyacid also explains the more pronounced desorption with decreasing electrode potential at elevated temperatures. It is obvious from Fig. 3 that, if the temperature is raised from $25 \, ^{\circ}C$ to 55 and $70 \, ^{\circ}C$, the maximum adsorption appears at less negative potentials (though the minimum is less pronounced for the data measured at 55 and $70 \, ^{\circ}C$). A likely explanation for this observation is a shift in the potential of zero charge with temperature in the studied system. However, no information on this effect could be found in the available literature. A further phenomenon is also apparent from the data, which confirms the presence of adsorption, namely a shift of the H_3PO_3 oxidation peak pα potential towards negative potential values with its increasing overall charge, see Fig. 2. If the peak were governed purely by the oxidation kinetics and the diffusion of electroactive species towards the electrode, the opposite shift would be expected.

The behaviour of H_3PO_3 in $0.5 \, mol \, L^{-1}$ $HClO_4$ electrolyte was comparable to that in H_2SO_4 solution, except for the intensities of the H_3PO_3 oxidation peaks. The peak charges in $HClO_4$ electrolyte at $25 \, ^{\circ}C$ were found to be approximately 40% higher than those observed in H_2SO_4 solution. This difference can be ascribed to stronger adsorption of SO_4^{2-} and especially HSO_4^{-} anions on the Pt electrode, in comparison to relatively inert ClO_4^{-}, which leaves lower number of surface sites available for H_3PO_3 adsorption. Fig. 4 clearly shows that the amount of H_3PO_3 adsorbed during polarisation in the H adsorption/evolution potential region at $25 \, ^{\circ}C$ was highest at a lower reversal potential of $-0.35 \, V$ (Fig. 4). This value again corresponds to the reported zero charge potential of polycrystalline Pt in $0.1 \, mol \, L^{-1}$ $HClO_4$ at $25 \, ^{\circ}C$ [25]. However, unlike in the H_2SO_4 solution, the desorbed amount of H_3PO_3 at $25 \, ^{\circ}C$ did not change dramatically until the lower reversal potential reached a value of $-0.6 \, V$, corresponding to the onset of H_2 evolution. This is due to the lack of competitive adsorption of the supporting electrolyte anion. Hence, in the $HClO_4$ electrolyte the adsorption of H_3PO_3 is negatively affected mainly below $-0.6 \, V$, i.e. by hydrogen adsorption in the H_2 evolution potential region. In the case of temperatures of 55 and $70 \, ^{\circ}C$ the dependence of the amount of desorbed H_3PO_3 on lower reversal potential is almost identical, which is slightly surprising. The desorbed amount of H_3PO_3 rises substantially when the lower reversal potential is
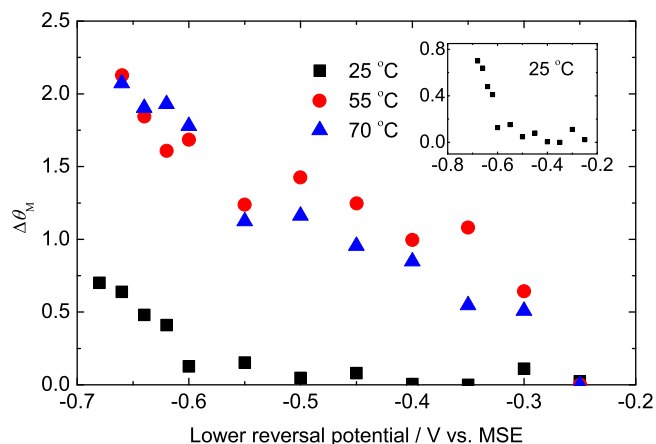
Fig. 4. Dependence of desorbed H_3PO_3 monolayers on lower reversal potential during cyclic voltammetry measurements in $0.5 \, mol \, L^{-1}$ $HClO_4$ aqueous solution with an addition of $1 \, mmol \, L^{-1}$ H_3PO_3 ($-0.25 \, V \rightarrow$ lower reversal potential $\rightarrow 0.84$ $V \rightarrow -0.25 \, V$), potential sweep rate $50 \, mV \, s^{-1}$. Electrolyte saturated with N_2. Electrolyte temperature is stated in the figure inset. Inserted plot shows detail of data recorded at temperature of $25 \, ^{\circ}C$.

decreased from −0.3 V to −0.6 V, where it attains a value of about 1.5 monolayers. Below −0.6 V the intensity of desorption again increases even more due to the hydrogen adsorption in the region of H_2 evolution and reaches a value of 2.2 monolayers at −0.66 V. This value of the total amount of H_3PO_3 desorbed at this potential is very similar for both supporting electrolytes studied, i.e. it does not seem to be influenced by the character of the anion.

3.2. Kinetics of H_3PO_3 oxidation

H_3PO_3 polarisation curves were obtained by potentiostatic sampling voltammetry at 25, 55 and 70 °C for H_3PO_3 concentrations of 0.2, 1 and 5 mmol L^{-1}. The voltammograms recorded at 25 °C are presented in Fig. 5. Oxidation of H_3PO_3 starts at around −0.05 V and the limiting current plateau can be found on the voltammograms. In the case of H_3PO_3 concentration of 5 mmol L^{-1}, the limiting plateau is not visible due to the formation of a PtO layer by which the mechanism of H_3PO_3 oxidation changes, as will be discussed later in section 3.4. An increase in temperature to 55 and 70 °C shifted the onset of H_3PO_3 oxidation to a more negative potential of around −0.1 V. At the same time the limiting plateau was significantly less pronounced than at 25 °C. This is especially apparent in the case of the solution containing 5 mmol L^{-1} H_3PO_3. To widen the kinetics-governed potential region of the polarisation curves mass transfer corrected currents were calculated according to Eq. (7) [9,26].

$$I_{corr} = \frac{I \cdot I_{lim}}{I_{lim} - I} \tag{7}$$

I_{corr}—mass transport corrected current in A, I—measured current in A, I_{lim}—average current in the limiting plateau of the polarisation curve in A.

The apparent charge transfer coefficient values determined, presented in Table 2, vary between 0.52 and 0.95. The values increase with both the rising temperature and the decreasing H_3PO_3 concentration in the electrolyte. It has been shown, e.g. by Holewinski et al., that in the presence of adsorption of species involved in the electrochemical reaction, the charge transfer coefficient value is not only a function of the position of the rate-determining step in the reaction mechanism, but also of the extent of adsorption of all species involved [27]. Since the extent of H_3PO_3 (and its oxidation intermediates) adsorption in the potential range of its oxidation is unknown, the charge transfer coefficient values are presented without a mechanistic interpretation. This will be the subject of future work.
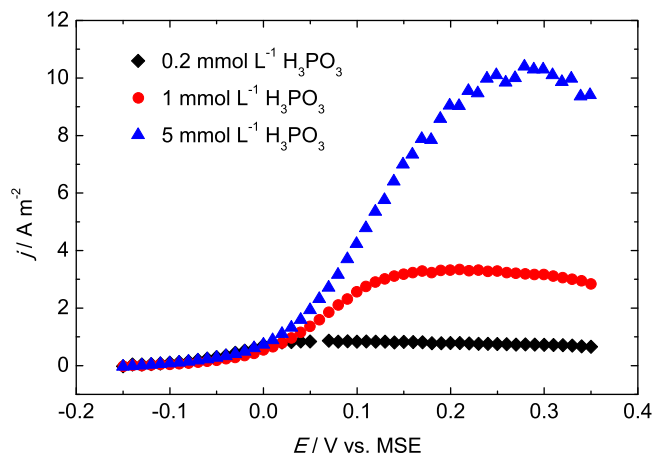

Fig. 5. Potentiostatic voltammetric curves of H_3PO_3 oxidation on a polycrystalline Pt electrode recorded at 25 °C in 0.5 mol L^{-1} H_2SO_4 with an addition of H_3PO_3. Electrolyte saturated with N_2. H_3PO_3 concentrations are stated in the plot inset.

Table 2
Temperature and concentration dependence of H_3PO_3 electrochemical oxidation charge transfer coefficient α and temperature dependence of apparent reaction order on a polycrystalline Pt electrode in 0.5 mol L^{-1} H_2SO_4 aqueous solution saturated with N_2. The Tafel equation is in the form E = $E_{logj=0}$ + logj(273.15 + T)R/(Fα).

	α			$E_{logj=0}$/V			reaction order
	c / mmol L^{-1}			c / mmol L^{-1}			
T / °C	0.2	1	5	0.2	1	5	
25	0.77	0.57	0.53	0.09	0.10	0.09	0.18
55	0.79	0.74	0.67	0.01	0.03	0.03	−0.11
70	0.95	0.75	0.68	−0.03	0.01	0.01	−0.04

The apparent reaction orders of H_3PO_3 electrochemical oxidation in the potential range of interest were determined from the dependence of current density at constant potentials on the logarithm of H_3PO_3 concentration. The slope of this dependence is the apparent order of reaction with respect to H_3PO_3. The current densities were read for each concentration and potential in the Tafel region of the polarisation curve. The calculated values of the reaction orders at 25, 55 and 70 °C are included in Table 2. With increasing temperature the reaction order of H_3PO_3 oxidation decreased from a value of 0.18 at 25 °C to −0.04 at 70 °C. This is in agreement with the above discussed dependence of H_3PO_3 adsorption on temperature because the rate of H_3PO_3 oxidation is not directly influenced by its bulk concentration. Instead, it is largely affected by the surface excess of H_3PO_3.

In the framework of this study an attempt was also made to determine the H_3PO_3 apparent diffusion coefficients, D_{app}, by integrating the current response obtained during polarisation measurements by the potential step measurements. In the method described earlier by Bard and Faulkner [28] the D_{app} is calculated from a linearised coulometric plot using Eq. (8). The data selected from the potential step measurements were located in the diffusion-limited area, thus permitting the effects of adsorption and double layer charging to be neglected.

$$Q(t) = nFAk_fc_r\left(\frac{2t^{1/2}}{H\pi^{1/2}} - \frac{1}{H^{1/2}}\right) \tag{8}$$

where

$$H = \frac{\pi^{1/2}}{2t_i^{1/2}} = \frac{k_f}{D_{app}^{1/2}} \tag{9}$$

$Q(t)$—charge in time in C, n—molar amount in mol, k_f—heterogenous rate constant of oxidation in m s^{-1}, c_r—concentration of H_3PO_3 in mol m^{-3}, t—time in s, t_i—time in s (obtained from the intercept of dependence Q vs. $t^{1/2}$ with x-axis), D_{app}—apparent diffusion coefficient of H_3PO_3 in m^2 s^{-1}.

The calculated D_{app} values are summarised in Table 3. The D_{app} values were found to be dependent on both the temperature and the concentration of H_3PO_3 in the electrolyte. As expected, D_{app} increases with rising temperature, namely at each concentration D_{app} is an approximately linear function of the temperature. However, D_{app} was found to change excessively with H_3PO_3 concentration. In particular, an increase in H_3PO_3 concentration

Table 3
Temperature and concentration dependence of H_3PO_3 apparent diffusion coefficient in 0.5 mol L^{-1} H_2SO_4 aqueous solution saturated with N_2.

T / °C	c / mmol L^{-1}			
	0.2	1	5	
25	0.63	0.26	0.05	D_{app} / 10^{-9} m^2 s^{-1}
55	2.62	1.52	0.43	
70	3.48	2.15	0.56	

from 0.2 to 5 mmol L^{-1} leads to a decrease in D_{app} by a factor of 10 at constant temperature. As a result, D_{app} values in the range of 10^{-9}–10^{-11} m^2 s^{-1} were calculated. It is obvious that these D_{app} values (especially at higher concentrations) have no physical meaning due to some process hindering electrode activity, especially at higher H$_3$PO$_3$ concentrations. A likely explanation is blockage of a substantial part of the Pt surface by slowly desorbing product (or H$_3$PO$_3$ oxidation intermediate) that effectively decreases the rate of H$_3$PO$_3$ anodic oxidation at the electrode. Most probably the H$_2$PO$_4^-$ anions produced at the electrode surface remain adsorbed on the Pt surface and are responsible for blocking its active sites. This hypothesis is supported by the fact that H$_2$PO$_4^-$ anions adsorb mainly at potentials roughly corresponding to those of H$_3$PO$_3$ oxidation [6].

3.3. H$_4$P$_2$O$_6$ electrochemical behaviour on a Pt electrode

The electrochemical behaviour of H$_4$P$_2$O$_6$ as a potential H$_3$PO$_3$ oxidation intermediate product was examined in 0.5 mol L^{-1} H$_2$SO$_4$ solution. The corresponding cyclic voltammograms are presented in Fig. 6. The addition of H$_4$P$_2$O$_6$ to 0.5 mol L^{-1} H$_2$SO$_4$ electrolyte caused a slight delay in PtO$_x$ formation. A peak related to H$_4$P$_2$O$_6$ electrochemical oxidation to H$_3$PO$_4$ was observed in the potential region of 0.4–0.7 V in all cases. This is well in the PtO$_x$ region, which shows that H$_4$P$_2$O$_6$ only oxidises on an already formed PtO$_x$ surface. Similar to H$_3$PO$_3$, H$_4$P$_2$O$_6$ oxidation requires a substantial overpotential to proceed, since the standard redox potential of H$_4$P$_2$O$_6$/H$_3$PO$_4$ couple is −1.587 V, see Eq. (2). The voltammograms in Fig. 6 allow one to conclude that H$_4$P$_2$O$_6$ has no impact on the electro-active surface area of Pt. Slight differences, especially visible on the voltammogram recorded in the presence of 10 mmol L^{-1} H$_4$P$_2$O$_6$ in the electrolyte, can be attributed to the effect of H$_3$PO$_3$ emerging in the electrolyte due to H$_4$P$_2$O$_6$ disproportionation, according to Eq. (1). This conclusion is supported by the appearance of a small oxidation peak around 0.1 V, corresponding to H$_3$PO$_3$ anodic oxidation. Such effects due to H$_4$P$_2$O$_6$ chemical decomposition are even more pronounced at elevated temperatures, see Fig. 7.

The electrochemical behaviour of H$_4$P$_2$O$_6$ was also examined in H$_3$PO$_4$ aqueous solution in order to evaluate the effect of H$_2$PO$_4^-$ anion on H$_4$P$_2$O$_6$ oxidation. The voltammograms measured in H$_2$SO$_4$ and H$_3$PO$_4$ solutions at 25 and 70 °C are compared in Fig. 7. In H$_3$PO$_4$ solution the oxidation peak of H$_4$P$_2$O$_6$ around 0.7 V was much less pronounced and its maximum shifted to more positive potentials than in H$_2$SO$_4$. The reason is stronger adsorption of
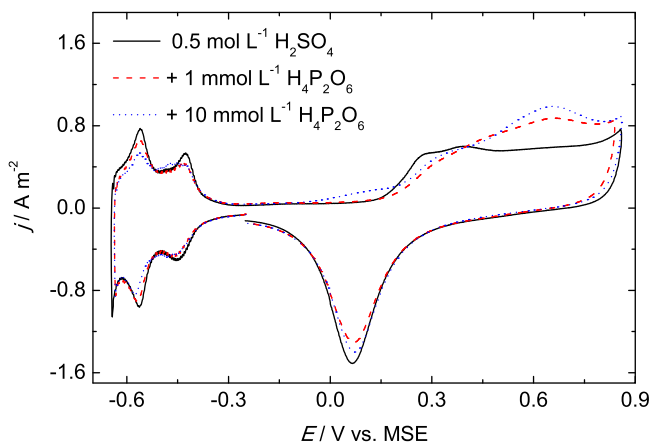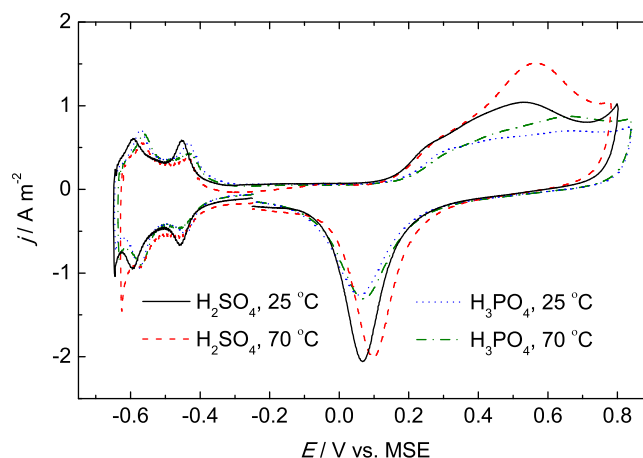
Fig. 7. Cyclic voltammograms of 1 mmol L^{-1} H$_4$P$_2$O$_6$ solution showing electrochemical behaviour on a polycrystalline Pt electrode in different 0.5 mol L^{-1} supporting electrolytes. Electrolyte saturated with N$_2$. Electrolyte compositions and temperatures used are included in plot inset.

H$_2$PO$_4^-$ compared to HSO$_4^-$ and consequently a lower electro-active area available for H$_4$P$_2$O$_6$ oxidation. The same effect is responsible for an approximately 50 mV shift of PtO$_x$ formation in H$_3$PO$_4$ solution to more positive potentials than in H$_2$SO$_4$ solution. On the other hand, the observed chemical decomposition of H$_4$P$_2$O$_6$ was much slower in H$_3$PO$_4$ than in H$_2$SO$_4$. This is understandable because of the substantial difference in acidity of the solutions (pH of 0.5 mol L^{-1} H$_2$SO$_4$ aqueous solution is 0.35 and that of 0.5 mol L^{-1} H$_3$PO$_4$ is 1.04). Thus, H$_4$P$_2$O$_6$ decomposes faster in H$_2$SO$_4$ solution due to its higher acidity. At the same time, H$_3$PO$_4$ is the final product of H$_4$P$_2$O$_6$ decomposition in an acidic environment, therefore its presence decreases the driving force of the disproportionation.

3.4. H$_3$PO$_3$ and H$_4$P$_2$O$_6$ oxidation on an oxidised Pt surface

Both compounds studied, i.e. H$_3$PO$_3$ and H$_4$P$_2$O$_6$, were found to be oxidised in the region of PtO$_x$ formation, where the parallel Pt surface oxidation complicates an analysis of the data. In order to elucidate the mechanism of these oxidation processes a series of chronopotentiometric experiments was performed. First, the Pt working electrode was oxidised at 0.6 V for 5 s and then a decrease in the open circuit potential (OCP) of the electrode was recorded. Oxidation of the electrode in pure 0.5 mol L^{-1} H$_2$SO$_4$ solution led to oxide coverage of approximately 60% (if PtO is assumed) of the electrode surface. The results of these experiments are presented in Fig. 8. OCP decay, observed after initial oxidation in 0.5 mol L^{-1} H$_2$SO$_4$, was slow and after 6000 s OCP attained a value of 0.19 V and further decreased. In this case, the decay of OCP can be explained by gradual dissolution of the PtO$_x$ layer in H$_2$SO$_4$ solution until a state of equilibrium between Pt/PtO$_x$ and Pt^{2+} in the solution is reached [29]. In order to ensure that this effect is not due to the oxidation of impurities in the electrolyte solution, it was treated with H$_2$O$_2$ prior to the experiements. H$_2$O$_2$ was consequently decomposed by heating in a closed vessel.

In the case of preoxidation in the presence of H$_3$PO$_3$ in the solution the passed charge was higher because at 0.6 V the anodic oxidation of H$_3$PO$_3$ takes place in parallel with PtO$_x$ formation. As a first approximation it was assumed that coverage by PtO$_x$ after preoxidation was comparable to the case of preoxidation without H$_3$PO$_3$. The presence of H$_3$PO$_3$ in the electrolyte led to a dramatic decrease in the OCP of the electrode after a few seconds of chronopotentiometric measurement and an OCP of −0.24 V was attained after 100 s of the experiment. This indicates fast chemical

Fig. 6. Cyclic voltammograms of H$_4$P$_2$O$_6$ solution showing electrochemical behaviour on a polycrystalline Pt electrode in 0.5 mol L^{-1} H$_2$SO$_4$ with an addition of H$_4$P$_2$O$_6$ at 25 °C. Electrolyte saturated with N$_2$. Electrolyte compositions are included in plot inset.
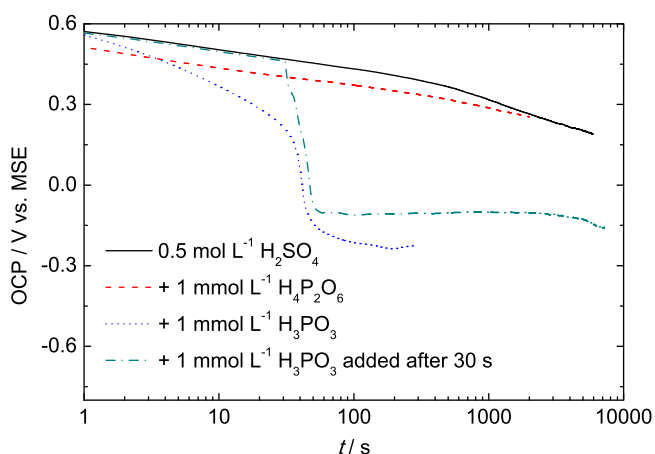
Fig. 8. Chronopotentiometric (I = 0) curves recorded on a polycrystalline Pt electrode at temperature 25 °C. 5 s electrode prepolarisation at E = 0.6 V. Supporting electrolyte 0.5 mol L^{-1} H$_2$SO$_4$ saturated with N$_2$. Electrolyte compositions are included in plot inset.

oxidation of H$_3$PO$_3$ on an oxidised platinum surface. In order to confirm that the observed rapid drop in OCP was not caused by an insufficient degree of Pt surface oxidation, a second measurement with H$_3$PO$_3$ was performed. This time the Pt was preoxidised in the absence of H$_3$PO$_3$ in the electrolyte, so initial surface coverage by PtO$_x$ was defined and not affected by H$_3$PO$_3$. It can be seen from Fig. 8 that the decay in OCP follows that previously observed in 0.5 mol L^{-1} H$_2$SO$_4$ solution. H$_3$PO$_3$ was added to the electrolyte solution after 30 s of chronopotentiometric measurement and OCP immediately decreased. Within 100 s OCP value stabilised at −0.1 V. This potential is slightly higher than in the case of preoxidation in the presence of H$_3$PO$_3$, indicating a different amount of PtO$_x$ on the electrode surface (most likely due to interference of O$_2$ absorbed into the electrolyte during the addition of H$_3$PO$_3$).

Unlike H$_3$PO$_3$, the presence of H$_4$P$_2$O$_6$ in the solution had almost no impact on the decay in OCP observed after the preoxidation period. The recorded results were comparable to those measured in pure H$_2$SO$_4$ solution, showing that H$_4$P$_2$O$_6$ is fairly stable in contact with a PtO$_x$ surface under the experimental conditions used. A minor difference is visible only within the first few seconds of the experiment when a decrease in OCP was relatively rapid in solution containing H$_4$P$_2$O$_6$, presumably due to the partial disproportionation of H$_4$P$_2$O$_6$ in an acidic enviroment with H$_3$PO$_3$ as one of the products. These results also suggest that H$_4$P$_2$O$_6$ oxidation previously discussed in the context of the voltammograms in Figs. 6 and 7 is electrochemical in nature. In other words, it proceeds by means of electron transfrer between the H$_4$P$_2$O$_6$ molecule and the electrode surface, not by a chemical reaction between H$_4$P$_2$O$_6$ and PtO$_x$ present on the electrode surface.

3.5. H$_3$PO$_3$ batch electrolysis

To examine the possibility that H$_4$P$_2$O$_6$ is formed as an intermediate product during H$_3$PO$_3$ oxidation, batch electrolysis experiments were performed. The electrolytes consisted of 0.5 and 5 mmol L^{-1} H$_3$PO$_3$ dissolved in 0.5 mol L^{-1} H$_2$SO$_4$ aqueous solution at 25 °C. Electrolysis was performed at a constant potential of 0.1 V. At this potential H$_3$PO$_3$ is anodically oxidised and PtO$_x$ has not yet formed on the electrode surface. Thus, the passed charge only corresponds to the electrochemical oxidation of H$_3$PO$_3$. Even though the electrolyte solution was stirred vigorously, the measured current density decayed very rapidly and 60 s after

the onset of electrode polarisation it reached a value of about 10% of the initial current density. Therefore, in order to ensure a reasonable average current density of the electrolysis, the potential was changed to −0.25 V for 1 s after each 60 s of electrode polarisation at a potential of 0.1 V. It is conceivable that, as the H$_4$P$_2$O$_6$ molecule contains a P—P bond, it would most likely form from H$_3$PO$_3$ oxidation intermediate products at a high concentration of H$_3$PO$_3$ at or near the electrode surface. The electrode potential value of −0.25 V was chosen so as to allow the adsorption of substantial amount of H$_3$PO$_3$ (as was discussed in section 3.1) and to avoid unnecessarily large charging currents during the potential step. This situation is similar to that observed during the chronoamperometric determination of D_{app}, discussed in section 3.2 and it corresponds to blockage of the electrode surface by (intermediate) H$_3$PO$_3$ oxidation products. From the changes in H$_3$PO$_3$ concentration, the amount of produced H$_3$PO$_4$, the value of anodic charge passed during electrolysis and assuming the transfer of 2 electrons per oxidised molecule of H$_3$PO$_3$, 100% selectivity for H$_3$PO$_3$ to H$_3$PO$_4$ oxidation and current efficiency of 99.9% were obtained for this process. As mentioned above, H$_4$P$_2$O$_6$ could not be oxidised at the electrode potential of 0.1 V applied during electrolysis. The hydrolytic disproportionation described by Eq. (1) is, under the conditions of electrolysis, a relatively slow process. This shows that, if a reasonable amount of H$_4$P$_2$O$_6$ were to be generated in the course of anodic electrolysis, it would have to be present in the electrolyte and both the current efficiency and the selectivity values of H$_3$PO$_3$ oxidation to H$_3$PO$_4$ as calculated above would be substantially lower. As a result, it can be summarised that H$_4$P$_2$O$_6$ is not the intermediate in H$_3$PO$_3$ oxidation to H$_3$PO$_4$.

4. Conclusion

It can be concluded that the electrochemical behaviour of H$_3$PO$_3$ on a Pt electrode is quite complex. First, the adsorption of H$_3$PO$_3$ on Pt electrode takes place. Its extent was found to depend on several parameters: besides temperature, it is mainly the electrode potential and nature of the supporting electrolyte anion. In particular, the adsorbed amount is highest at the electrode potential near the potential of zero charge of the surface and in the non-adsorbing supporting electrolyte solutions such as HClO$_4$. The adsorbed amount of H$_3$PO$_3$ drops in H$_2$SO$_4$ electrolyte solutions (due to co-adsorption of supporting electrolyte anions) and at potentials of hydrogen underpotential deposition and in the hydrogen evolution region (adsorption of hydrogen). At temperatures above room temperature the adsorbed amount exceeds that corresponding to monolayer coverage and it is probable that, besides H$_3$PO$_3$, species like H$_4$P$_2$O$_5$ and H$_5$P$_3$O$_7$ are present at the electrode interface.

Secondly, H$_3$PO$_3$ can be oxidised on both a metallic Pt surface and a PtO$_x$ surface. While in the former case the reaction proceeds electrochemically via electron removal from a H$_3$PO$_3$ molecule, in the latter case it involves chemical oxidation of H$_3$PO$_3$ by PtO$_{x,surf}$. The anodic charge transfer coefficient of the process was found to depend on the bulk concentration of H$_3$PO$_3$ and the temperature of the electrolyte solution. It seems that the desorption of an oxidation (intermediate) product (most likely H$_2$PO$_4^-$) from the Pt surface is a fairly slow process. As a result, it accumulates on the Pt surface and substantially reduces the rate of the overall oxidation process.

In this work the electrochemical behaviour of hypophosphoric acid, H$_4$P$_2$O$_6$, was also studied. In contrast to H$_3$PO$_3$, H$_4$P$_2$O$_6$ behaves like a fairly inert compound. It neither adsorbs on the Pt surface nor does it react with Pt oxides, and its oxidation proceeds only on a preoxidised Pt surface by means of electron transfer. Using batch electrolysis it was confirmed that H$_4$P$_2$O$_6$ does not

form in detectable amounts during H_3PO_3 anodic oxidation at a Pt electrode at ambient temperature in H_2SO_4 electrolyte solution.

Though the presented results of H_3PO_3 adsorption and electrochemical oxidation were obtained at conditions far from these present in the HT PEM FC environment, they can still shed some light on the nature of the processes taking place in HTP EM FC during its operation. It also becomes clear that better understanding the phosphorus compounds behaviour is fundamental for better understanding of the processes occuring at the HT PEM FC during its operation.

Acknowledgement

References

[1] J. Andrews, B. Shabani, Re-envisioning the role of hydrogen in a sustainable energy economy, International Journal of Hydrogen Energy 37 (2012) 1184–1203.

[2] J. Zhang, Z. Xie, J. Zhang, Y. Tang, C. Song, T. Navessin, Z. Shi, D. Song, H. Wang, D. P. Wilkinson, Z.-S. Liu, S. Holdcroft, High temperature PEM fuel cells, Journal of Power Sources 160 (2006) 872–891.

[3] Q. He, X. Yang, W. Chen, S. Mukerjee, B. Koel, S. Chen, Influence of phosphate anion adsorption on the kinetics of oxygen electroreduction on low index Pt (hkl) single crystals, Physical chemistry chemical physics: PCCP 12 (2010) 12544–12555.

[4] K.-L. Hsueh, E.R. Gonzales, S. Srinivasan, D.T. Chin, Effects of phosphoric acid concentration on oxygen reduction kinetics at platinum, J. Electrochem. Soc. 131 (1984) 823–828.

[5] S. Kaserer, K.M. Caldwell, D.E. Ramaker, C. Roth, Analyzing the influence of H3PO4 as catalyst poison in high temperature PEM fuel cells using in-operando X-ray absorption spectroscopy, The Journal of Physical Chemistry C 117 (2013) 6210–6217.

[6] F.C. Nart, T. Iwasita, On the adsorption of H2PO4- and H3PO4 on platinum: An is situ FT-ir study, Electrochimica acta 37 (1992) 385–391.

[7] W.M. Vogel, J.M. Baris, Changes in the surface of platinum in hot concentrated phosphoric acid at low potentials, Electrochimica Acta 23 (1977) 463–466.

[8] R. Jasinski, J. Huff, S. Tomster, L. Swette, Electrochemical oxidation of hydrocarbons, Berichte der Bunsengesellschaft 68 (1964) 400–404.

[9] S.J. Clouser, J.C. Huang, E. Yeager, Temperature dependence of the Tafel slope for oxygen reduction on platinum in concentrated phosphoric acid, Journal of applied electrochemistry (1993) 597–605.

[10] N. Sugishima, J.T. Hinatsu, F.R. Foulkes, Phosphorous acid impurities in phosphoric acid fuel cell electrolytes: I. Voltammetric study of impurity formation, Journal of The Electrochemical Society 141 (1994) 3325–3331.

[11] M. Prokop, T. Bystron, K. Bouzek, Electrochemistry of Phosphorous and Hypophosphorous Acid on a Pt electrode, Electrochimica Acta 160 (2015) 214–218.

[12] N. Sugishima, J.T. Hinatsu, F.R. Foulkes, Phosphorous acid impurities in phosphoric acid fuel cell electrolytes: II. Effects on the oxygen reduction reaction at platinum electrodes, Journal of The Electrochemical Society 141 (1994) 3332–3335.

[13] W.H. Doh, L. Gregoratti, M. Amati, S. Zafeiratos, Y.T. Law, S.G. Neophytides, A. Orfanidi, M. Kiskinova, E.R. Savinova, Scanning photoelectron microscopy study of the Pt/phosphoric-acid-imbibed membrane interface under polarization, ChemElectroChem 1 (2014) 180–186.

[14] J. Bravacos, M. Bonnemay, E. Levart, A.A. Pilla, Contribution á l'étude du systéme électrochimique platine-acide phosphorique, C.R. Acad. Sc. Paris 265 (1967) 336–340.

[15] S. Trasatti, A. Alberti, Ossidazione anodica degli acidi ipofosforoso e fosforoso su palladio e platino, La Ricerca Scientifica 8 (1965) 1012–1025.

[16] Y.V. Babin, A.V. Prisyazhnyuk, Y.A. Ustynyuk, The dynamic structure of cis and trans conformers of substituted phosphinous acids, Russian Journal of Physical Chemistry B 2 (2009) 684–689.

[17] J.P. Guthrie, Tautomerization equilibria for phosphorous acid and its esters, free energies of formation of phosphorus and phosphonic acids and their ethyl esters, and pKa values for ionization of the P-H bond in phosphonic acid and phosphonic esters, Can. J. Chem. 57 (1979) 236–239.

[18] G. Manca, M. Caporali, A. Ienco, M. Peruzzini, C. Mealli, Electronic aspects of the phosphine-oxide → phosphinous acid tautomerism and the assisting role of transition metal centers, Journal of Organometallic Chemistry 760 (2014) 177–185.

[19] V.M. Baudler, D. Schellenberg, Elektrolytische Untersuchungen von Phosphorsauren in wasriger Losung, Zeitschrift fur anorganisehe und allgemeine Chemie 340 (1965) 113–224.

[20] 12—Phosphorus, in: N.N. Greenwood, A. Earnshaw (Eds.) Chemistry of the Elements (Second Edition), Butterworth-Heinemann Oxford, 1997, pp. 473–546.

[21] S. Trasatti, A. Alberti, Anodic oxidation mechanism of hypophosphorous and phosphorous acid on palladium, Journal of Electroanalytical Chemistry 12 (1966) 236–249.

[22] S. Černý, M. Smutek, F. Buzek, The Calorimetric Heats of Adsorption on Platinum Films, Journal of Catalysis 38 (1975) 245–256.

[23] W. Dong, V. Ledentu, P. Sautet, A. Eichler, J. Hafner, Hydrogen adsorption on palladium: a comparative theoretical study of different surfaces, Surface Science 411 (1998) 123–136.

[24] H. Remy, H. Falius, Uber das Verhalten der Unterphosphorsaure, Naturwiss 43 (1956) 1.

[25] Q.-S. Chen, J. Solla-Gullón, S.-G. Sun, J.M. Feliu, The potential of zero total charge of Pt nanoparticles and polycrystalline electrodes with different surface structure: The role of anion adsorption in fundamental electrocatalysis, Electrochimica Acta 55 (2010) 7982–7994.

[26] M.M. Ghoneim, S.J. Clouser, E. Yeager, Oxygen Reduction Kinetics in Deuterated Phosphoric Acid, J. Electrochem. Soc. 132 (1985) 1160–1162.

[27] A. Holewinski, S. Linic, Elementary Mechanisms in Electrocatalysis: Revisiting the ORR Tafel Slope, Journal of the Electrochemical Society 159 (2012) H864–H870.

[28] A.J. Bard, L.R. Faulkner, Electrochemical methods: Fundamentals and applications, 2nd ed., John Wiley & Sons, USA, 2001.

[29] Y. Furuya, T. Mashio, A. Ohma, M. Tian, F. Kaveh, D. Beauchemin, G. Jerkiewicz, Influence of Electrolyte Composition and pH on Platinum Electrochemical and/or Chemical Dissolution in Aqueous Acidic Media, ACS Catalysis 5 (2015) 2605–2614.